



HAL
open science

A theoretical approach for elastically driven cooperative switching of spin crossover compounds impacted by an ultrashot laser pulse

Cristian Enachescu, Roman Stoleriu, Masamichi Nishino, Seiji Miyashita, Roman Stancu, Maciej Lorenc, Roman Bertoni, Hervé Cailleau, Eric Collet

► **To cite this version:**

Cristian Enachescu, Roman Stoleriu, Masamichi Nishino, Seiji Miyashita, Roman Stancu, et al.. A theoretical approach for elastically driven cooperative switching of spin crossover compounds impacted by an ultrashot laser pulse. *Physical Review B*, 2017, 95 (22), pp.224107. 10.1103/PhysRevB.95.224107 . hal-01552083

HAL Id: hal-01552083

<https://hal.science/hal-01552083>

Submitted on 30 Jun 2017

HAL is a multi-disciplinary open access archive for the deposit and dissemination of scientific research documents, whether they are published or not. The documents may come from teaching and research institutions in France or abroad, or from public or private research centers.

L'archive ouverte pluridisciplinaire **HAL**, est destinée au dépôt et à la diffusion de documents scientifiques de niveau recherche, publiés ou non, émanant des établissements d'enseignement et de recherche français ou étrangers, des laboratoires publics ou privés.

A theoretical approach for elastically driven cooperative switching of spin crossover compounds impacted by an ultrashort laser pulse

Cristian Enachescu*,¹ Laurentiu Stoleriu,¹ Masamichi Nishino,² Seiji Miyashita,³
Alexandru Stancu,¹ Maciej Lorenc,⁴ Roman Bertoni,⁴ Hervé Cailleau,⁴ and Eric Collet⁴

¹*Faculty of Physics, Alexandru Ioan Cuza University of Iasi, Romania*

²*International Center for Materials Nanoarchitectonics,*

National Institute for Materials Science, Tsukuba, Ibaraki, Japan

³*Department of Physics, Graduate School of Science,*

The University of Tokyo, Bunkyo-Ku, Tokyo, Japan

⁴*Univ Rennes 1, CNRS, UBL, Institut de Physique de Rennes (IPR) - UMR 6251, Rennes, France*

(Dated: April 30, 2017)

In this paper we use an elastic model in order to study the elastically driven cooperative switching of spin crossover materials after femtosecond laser excitation. In this model, the molecules occupy a triangular lattice in open boundaries systems and are connected by springs. The volume change of a molecule between its two possible spin states, low-spin and high-spin, determines a variation of the spring length and therefore induces elastic interactions between molecules, which propagates throughout the whole sample as elastic distortions. This model is able to reproduce the multi-step out-of-equilibrium response to ultrashort laser excitation and especially the elastically-driven cooperative response. Then this model is developed in order to predict the behaviour of the system as a function of its different physical parameters, such as the magnitude of the elastic constant or the homogeneity of the photoexcitation. The contribution of the reorganisation of the molecular states during elastic steps, leading to clusters of high-spin molecules towards edge or corners is also revealed.

PACS numbers: 75.30.Wx, 64.60.-i, 75.60.-d

I. INTRODUCTION

Spin crossover inorganic compounds are among the few systems showing bistability at a molecular scale with switchable properties by variations of temperature and pressure or by light irradiation^{1,2}. Pulsed laser irradiation opens the possibility to control this bistability in an ultrafast way, through strongly out-of-equilibrium conditions³⁻⁸. Their molecular switching occurs between the paramagnetic low spin state (*LS*), stable at low temperatures and paramagnetic high spin (*HS*) state of higher entropy, stable at higher temperature. Remarkably, not only magnetic and optical properties are different in the two states, but also the molecular volume, being around 3% higher in the *HS* state due the occupancy of antibonding ligand orbitals in *HS* molecules⁹. This size changes during thermal conversion between *LS* and *HS* states induces elastic interactions mediated by the lattice, which, if high enough, are responsible for abrupt transitions and cooperativity phenomena. At low temperatures, such crystals can be photo-switched from the ground *LS* state to the long-lifetime metastable *HS* state. By exciting some specific charge transfer bands, with a broad band lamp or a laser, the so called Light Induced Excited Spin State Trapping – LIESST effect – occurs^{10,11}. At long time scales, varying from nanosecond to days as a function of compound and temperatures,

the metastable *HS* state relaxes towards the ground state by a nonadiabatic, nonradiative process, either via tunnelling – at low temperature - or thermally activated process¹². The recent experiments using femtosecond laser for photoexcitation and the detailed analysis of the subsequent evolution of the system allowed the study of very fast dynamical phenomena and contributed to a better understanding of the behaviour of spin crossover compounds at molecular level^{5,13,14}. Observations of molecules in solutions or in solid compounds demonstrated that the photoswitching from the *LS* towards the *HS* states, involving both change of electronic states and molecular structural reorganization occurs within ≈ 200 fs¹⁵⁻¹⁸. In solids, this initial photo-switching of few molecules from *LS* to *HS* states triggers further increases of the fraction of *HS* molecules X_{HS} . This elastically driven cooperative switching of spin crossover compounds occurs due to the propagation of the elastic distortions in the medium, the superposition of which induces volume expansion of the lattice. This so-called elastic step⁵ during the of the out-of-equilibrium response following fs laser excitation, takes place on the acoustic time scale, which corresponds to the ratio between relevant size scale of the sample and the sound velocity in the medium.

The photoresponse measured through the time evolution of the fraction X_{HS} of *HS* molecules, is directly probed by ultrafast spectroscopy. Figure 1 shows typical photoresponse to fs laser excitation of SCO nanocrystals of $[Fe^{III}(3-MeO-SalEen)]PF_6$, which was reported in detail in ref.⁵. It is non-linear with excitation density. The fraction of molecules switched by light from

*Electronic address: cristian.enachescu@uaic.ro

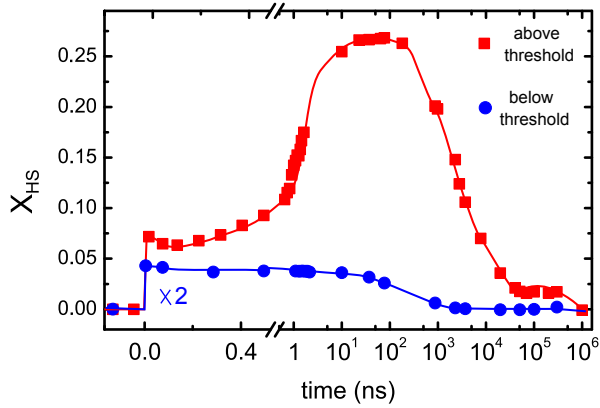


FIG. 1: Experimental evidence of the elastic step. The time course of X_{HS} following femtosecond laser excitation depends on the initial fraction of photoexcited molecules. For 2% (scaled $\times 2$) of photoexcited molecules a relaxation occurs within 1 μ s. For 7% a self-amplification occurs up to 27% within 1 ns during the elastic step.

LS to HS states $X_{HS}^{h\nu}$, measured at the picosecond time scale, depends linearly on the excitation density because of the local nature of the photoswitching process and each photon switches a single molecule. When the fraction of photoswitched molecules from LS to HS state is below 3%, the LS ground state is recovered within $\sim 1 \mu$ s. At higher excitation density the HS fraction increases. For high excitation density, the molecular swelling overcome the lattice pressure and drives its expansion, favouring so the HS state of higher volume. In this case a self-amplified transformation is observed and, in average, up to 7 molecules are switched per photon. The additional conversion on the elastic step is then defined as $\Delta X_{HS} = X_{HS}^{El} - X_{HS}^{h\nu}$. Therefore below the amplification threshold $\Delta X_{HS} < 0$, whereas above $\Delta X_{HS} > 0$.

Among the many models elaborated for the study of spin crossover compounds, elastic models^{19–23} are the more suitable for the study of the elastic step, as they build on the common sense by which interactions between molecules are of elastic origin and stem from the size difference between HS and LS molecules. Here we use a dynamic mechanoelastic model^{23–25} applied for open boundary systems in order to emulate the evolution of the system after femtosecond excitation as function of several parameters. Ab-initio models are useful for study the details of electronic and bonding states^{26,27}, but for studies of phase change, the mechano-elastic model and other spin-crossover elastic models have advantage. Especially for the phenomena of elastic step, the combination of molecular dynamics and stochastic dynamics, treated in this study, is effective. This model was briefly introduced in ref.⁵ and in the present paper we discuss the role of different parameters in the model and the resulting dynamics due to two competing and opposite going processes, namely the local relaxation and the non-local amplification.

II. THE MODEL

In the mechanoelastic model, the spin-crossover molecules are represented as rigid spheres, situated in triangular configurations in open boundary lattices and interacting through connecting springs, with the elastic constant k . The conversion between the two states, HS and LS , is accompanied by a variation of the volume of a switching molecule, producing an instantaneous elastic force in its neighboring springs, which is transferred, step by step, to all the molecules in the system, in a degree depending on their relative position from the switched molecule. Therefore, the volume and the shape of the whole system dynamically change with every molecular switch, as elastic deformation propagates through the sample.

The motion of molecules is determined by local elastic forces and is accounted by solving the following differential equations for all molecules in the system, for a specific number of steps n_1 .

$$\begin{cases} m \frac{d^2 x_i}{dt^2} = F_{i,x} - \mu \frac{dx_i}{dt} \\ m \frac{d^2 y_i}{dt^2} = F_{i,y} - \mu \frac{dy_i}{dt} \end{cases}, \quad (1)$$

where x_i, y_i are Cartesian coordinates of the molecule i , m is the mass of the molecule, μ is a damping constant, and $F_{i,x}, F_{i,y}$ the components of the instantaneous force acting on molecule i given by the sum of the forces from the neighbouring springs:

$$\begin{cases} F_{i,x} = \sum_{\text{neighbor springs}} k \delta r_{ij,x} \\ F_{i,y} = \sum_{\text{neighbor springs}} k \delta r_{ij,y} \end{cases}, \quad (2)$$

where δr_{ij} is the deviation of the neighbour spring j from its unstressed value. In order to study dynamical properties of the system during a spin transition within the ME model, one assigns for every spin-crossover molecule a $HS \rightarrow LS$ and a $LS \rightarrow HS$ transition probability, depending on the temperature T , on intrinsic molecular parameters (the $HS - LS$ energy difference D , the degeneracy ratio g , the effective activation energy E_A) and on the elastic interactions between molecules, represented here by the local pressure p_i acting on molecule i , defined as $p_i = \sum_{\text{neighbor springs}} \frac{k}{A} \delta r_{ij}$, with A the molecular cross-sectional area. These Arrhenius-type probabilities can be written as:

$$P_{HS \rightarrow LS}^i = \frac{1}{\tau} \exp\left(-\frac{E_A - \kappa p_i}{k_B T}\right) \quad (3a)$$

$$P_{LS \rightarrow HS}^i = \frac{1}{\tau} \exp\left(-\frac{D - k_B T \ln g}{k_B T}\right) \exp\left(-\frac{E_A + \kappa p_i}{k_B T}\right) \quad (3b)$$

where τ is a constant scaling factor, and κ a constant that relates the local pressure with the activation energy. We consider here that compressed springs produce a positive pressure (favouring the *LS* state), while elongated springs produces a negative pressure (favouring the *HS* state). After a Monte-Carlo standard procedure, one decides if a molecule switches or not. A Monte-Carlo electronic step (MCES) is completed when every molecule has been checked once, by comparing its transition probability (3a) or (3b) with a random number $\eta \in (0, 1)$. A given molecule changes its state only if this number is smaller than the corresponding probability. After each MCES, the new equilibrium positions of all molecules are found.

In order to tune the different relative time scales of spin dynamics and lattice relaxation, we define the ratio $r = \frac{n_1}{n_2}$, where n_1 is the number of steps to solve differential equations (1), with probabilities (3) fixed and n_2 is the number of MCES per n_1 . It should be noted that a large r (large n_1) favours equilibrium distribution, allowing to accommodate to the distribution of local pressure p_i , before any such pressure is changed, as previously considered in mechanoelastic model for reproducing static phenomena. It is in this way that the thermal hysteresis shown in figure 2, or slow relaxation curves²⁸ are simulated. Oppositely, a smaller r (high n_2) favours non-equilibrium distribution when the probabilities (3) change before the system accommodates to the distribution of local pressure, like in the case of fast phenomena subsequent to femtoseconds photoexcitation experiments²⁹. This is due to the fact that molecular switching timescale (related to n_1) characterized by the timescale related to intra-molecular bond expansion (200 fs) is shorter than the typical lattice equilibration timescale (ns). In this paper, if not stated otherwise, we have used $r = 1$, that means that we solve one single step of differential equations after every MCES. This value corresponds to a situation when the lattice relaxation timescale is much longer than the molecular switching timescale.

For the present simulations, we use a rectangular shape sample, composed of 13982 molecules in triangular configurations which translates into real space in a $60 \text{ nm} \times 60 \text{ nm}$ sample for the typical value of 1 nm per molecule. The value of the parameters considered in the simulations are in the range of those found by the estimation of the variation of the ligand field strengths in the two spin states due to the cooperativity and the bulk modulus³⁰: $\kappa = 0.2 \times 10^{-10} \text{ A m}$, $k = 5 \text{ N m}^{-1}$, with the bond-length difference between the *HS* and

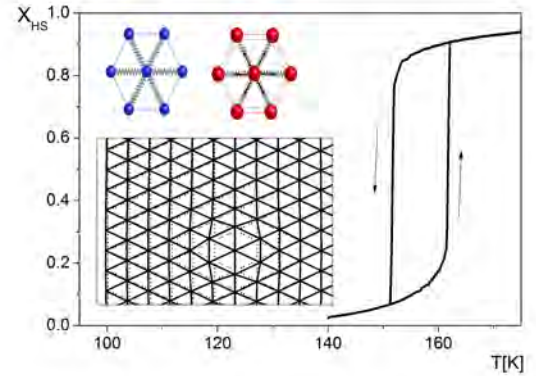


FIG. 2: (main figure) Typical dynamical *LS*–*HS* transformation at 10000 MC steps/K; (inset) (up) *LS* molecule in *LS* environment and *HS* molecule in *HS* environment (down) The triangular network of particles connected with springs. In the initial state all the molecules are in the *LS* state (open circles). When a molecule switches its state to *HS* (red full circle), all the other molecules (small circles) change their positions. The lattice becomes then distorted: the distortions are bigger in the vicinity of switched molecule (short range effect), but they are present even in remote parts of the system (long range effect).

LS molecules $\Delta r_{HL} = 0.2 \times 10^{-10} \text{ m}$, while other parameters are $\mu = 0.7 \text{ N s m}^{-1}$, $E_A = 552 \times 10^{-23} \text{ J}$, $\Delta H = 1520 \times 10^{-23} \text{ J}$ and $g = 1096$, thus giving a thermal transition temperature $T_{1/2} = \Delta H / k_B \ln g$ of around 157 K (figure 2) close to the one experimentally reported for $[\text{Fe}^{III}(\text{3-MeO-SalEen})]\text{PF}_6$.

We consider a temperature below the thermal transition temperature, at which most of the molecules are in the *LS* state. First, we run enough Monte Carlo steps in order to find the steady state at the corresponding temperature. Then the homogenous photoexcitation is simulated by choosing randomly a number of *LS* molecules, corresponding to the desired photoexcitation percentage, and by switching them to the *HS* state. Simultaneously, their individual temperature is increased with $\Delta T = 100 \text{ K}$ ³¹. This value is in line with the lattice heating experimentally observed of 15-20 K for a 15-20% photoexcitation. (consequently if 20% photoexcitation results in a global system heating of around 20 K, after the energy redistribution, we may assume that a 100% photoexcitation will result in a 100 K global heating, and, for practical purposes in Monte Carlo algorithm, we assume this value as individual increase of temperature for every photoexcited molecule). The temperature increase on the excited molecule allows to reduce the relaxation process towards its initial *LS* state due to lattice pressure. Here, as we are interested to simulate the behavior of the system for short time after photoexcitation when the elastic step appears and consider that the thermal diffusion is negligible and all molecules keep constant their temperatures attributed after the photoexcitation. This

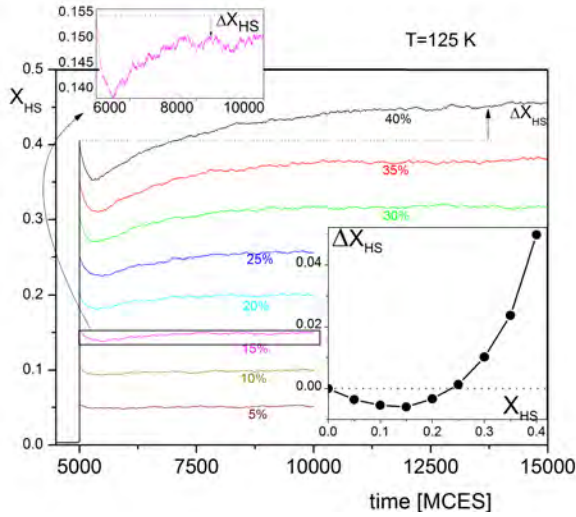


FIG. 3: Simulation of the evolution of the HS fraction after different percentages of photoexcitation showing the elastic step. Inset: the variations of ΔX_{HS} after the elastic step as a function of photoexcitation ratio at constant $T = 125$ K.

approximation was made for avoiding thermally-induced switching due to laser heating. We have also performed calculations taking into account the energy redistribution between the photoexcited molecules and their environment and, qualitatively, the same effects are observed. However, a correct description of the heat diffusion is more complex and this will be a further step towards more realistic simulations. Even if the heat diffusion could occur really quick for a high excitation (distance between two excited LS), the energy barriers between LS and HS are such that Arrhenius-like conversion takes much longer than the arrival of the elastic step³². Then, the system is allowed to evolve without any external influence by alternative checking molecules for switching and solving the system of differential equations.

The dependence of ΔX_{HS} on the initial photoexcitation percentage is shown in figure 3 for a constant temperature $T = 125$ K. If the photoexcitation percentages are high enough, we notice a fast relaxation after the photoexcitation, followed by an increase of the HS fraction, which eventually surpasses the initial photoexcitation as observed experimentally. The variation of the HS fraction between the elastic step and after photoexcitation is ΔX_{HS} (figure 1). However, if the initial photoexcitation percentage is too small, only the relaxation from HS to LS states can be observed and $\Delta X_{HS} < 0$. The apparent trough at $\Delta X_{HS} = 0.15$ is the manifestation of two competing and opposite going processes, namely the local relaxation and the non-local amplification.

The dependence of ΔX_{HS} with temperature for a photoexcitation percentage of 15%, is shown in figure 4. If the temperature is close to the thermal transition temperature, then a large increase in the HS fraction is observed after photoexcitation. This increase corresponds to the

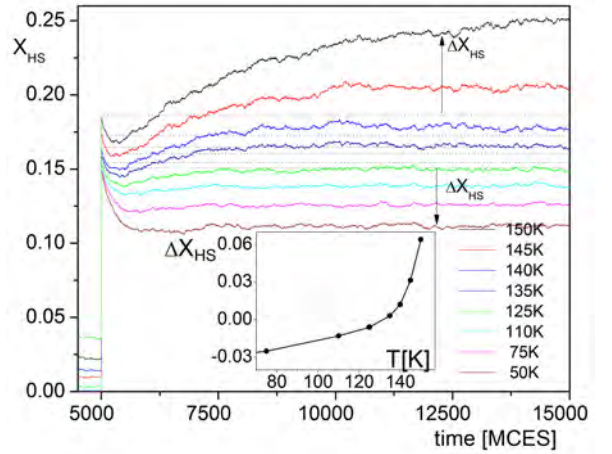


FIG. 4: Simulation of the evolution of the HS fraction after photoexciting 15% of LS molecules showing the elastic step at different temperatures. Inset: the variations of ΔX_{HS} after the elastic step as a function of temperature.

experimentally observed elastic step⁵. The amplitude of this elastic step decreases with decreasing temperature until it vanishes at around 125 K. For temperatures below 125 K, only the relaxation subsequent to photoexcitation can be observed. By depicting the threshold at $\Delta X_{HS} = 0$, figure 4 (inset), we can conclude that with increasing the temperature, which stabilizes the higher entropy HS state, and thus the equilibrium HS fraction, the elastic step takes on a greater magnitude. This could be rationalized with the lattice getting softer, which requires less elastic cost for macroscopic volume expansion and molecular switching.

We plot in figure 5 the variation of the volume (that actually in our 2D case is just the area S) of the whole sample at 145 K for two opposite cases, showing or not the elastic step. As it takes some time for stress inside the lattice to propagate via an elastic distortion towards the edges of the system, the volume (area) variation does not exactly follow the X_{HS} variation. In both cases, the initial HS fraction relaxation cannot be detected by the area variation: while some of the HS molecules relax, the area, which still corresponds to a state configuration before the photoexcitation, starts to increase in order to match the updated state due to internal pressure. Even in the case where only the relaxation is observed, the area still increases, as it should fit a state with ΔX_{HS} higher than prior to photoexcitation. We should strengthen here that at short times described by our simulations only the propagation of phonons, driven by a harmonic-type potential influence the switch of molecules all around the sample, as the heating transfer between molecules is neglected and all of them keep their temperature. Only in case of high value of r , the area and the fraction would be somewhat artificially brought to concur in time. We emphasize that in our calculations $r = 1$, which corre-

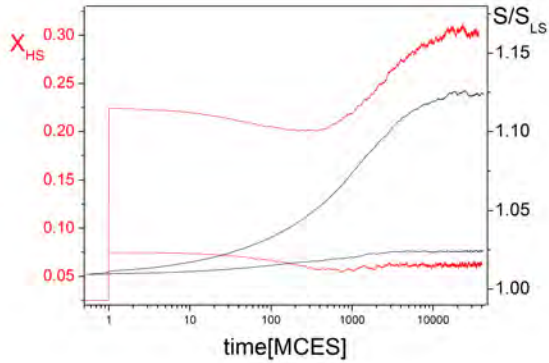


FIG. 5: Variation of X_{HS} and of total area during elastic step at 145 K after two different initial photoexcitation percentages.

sponds to a realistic value that allowed reproducing all features on experimentally determined timescales.

The explanation of the experimental observation is strictly related to the microscopic evolutions inside the material, as it results from figure 6, where we present snapshots of the system taken at 145 K at different instants, before and during the elastic step. In figure 6 upper left, we show the situation just after photoexcitation, once molecules have switched from LS to HS state of higher volume but before the lattice relaxation starts. With this random distribution of HS molecules in a frozen lattice, most of them experience a very high pressure applied on them (blue circles). This high pressure will determine the switching back of several HS molecules to the lower volume LS state. Only the fact that the temperature of the photoexcited molecules has been increased prevents the switching back of all HS molecules (3). After a while (just at the end of relaxation part of X_{HS}), the relaxation of the lattice leads to a decreasing of pressure for molecules situated closer to the edge (red and black circles). This state is associated with the end of the relaxation part of the curves. Remarkably, the molecules still associated with a high pressure are situated inside a circular area, just in the middle of the sample. This observation shows actually how the relaxation starts from the edges, developing towards the center. Later on, during the elastic step, the lattice has almost completely relaxed. There are no more molecules with a high pressure acting on them, while the number of the molecules with a low pressure and in the HS state increased, especially towards edges and corners (black circles). This situation corresponds to figure 6.f, where one shows a "reorganized" sample: accumulations of HS molecules (small clusters) are concentrated towards corners and edges. Actually, this figure helps us to understand the nature of the elastic step. Several photoexcited molecules situated in the vicinity of corners / edge will lead to local deformations of the lattice resulting in creating more space for nearby LS molecules.

This means that most springs around the LS molecules will be elongated and, therefore, the $LS - HS$ switching probability for these molecules will increase, and many of them will switch to HS state. Therefore, the elastic step appears due to a reorganization of the molecules with different spin state and volume in the vicinity of corners / edges [movie in the Supplemental Material³³]. The same conclusions can be drawn from the representations of the maps of local pressures, i.e. compressions or elongations of every spring in the system, which are similar to local deformation fields in a continuous medium, as shown in Figure 7. Just after photoexcitation, the values of the local pressures are homogeneously distributed all around the sample, with somewhat larger values around photo-switched molecules (Fig. 7, a); then high local pressures persists for a while in a central region of the sample, while they decrease faster for edges (fig. 7, b, c). Towards the end of the elastic step, the local pressures are again homogenous all around the sample, but with lower values. (Fig. 7, e, f). a,b,c,d,e,f correspond to different MCES shown in Figure 8.

The results presented in figure 8 supports these statements. They show, separately, the evolution of X_{HS} for regions in the middle of the sample and towards the edge and support the hypothesis that most of the effect is due to the increase of the number of HS molecules towards the edge. While towards the edges there is almost no decrease of X_{HS} after irradiation (as the additional pressure is rapidly freed by the increase of the volume), in the inside part the relaxation is important and the average of X_{HS} is much smaller than for the whole sample. In the inset of figure 8, we present the variation of local pressures values during the elastic step. As qualitatively shown in figure 7, they decrease faster at the edges of the sample and slower in the bulk, but stabilize in the whole sample around the same non-null value towards the end of the elastic step.

The next question is to study the influence of the elastic constant on the magnitude of the elastic step. To clarify this point, we have simulated the behaviour of the system keeping constant all parameters of the system (as mentioned before), except the elastic constant. The temperature (145 K) and the photoexcitation percentage (20%) is also similar for all simulations. The results are presented in figure 9. At first sight, it can be stated that the elastic step exists even for smaller values of the elastic constant, when no hysteresis appears and that there is no monotonic evolution of the magnitude of the elastic step with the amplitude of the elastic constant (a maximum value of the elastic step is obtained for an intermediate elastic spring value). However, due to the different steady state before photoexcitation (see figure 9 inset), the interpretation of these results is rather difficult, as we have previously shown, the value of the elastic step depends also on the initial photoexcitation state. On one side, these results show the existence of an elastic step independently of the value of k , while we may imagine a chemical tuning of a material in order to obtain

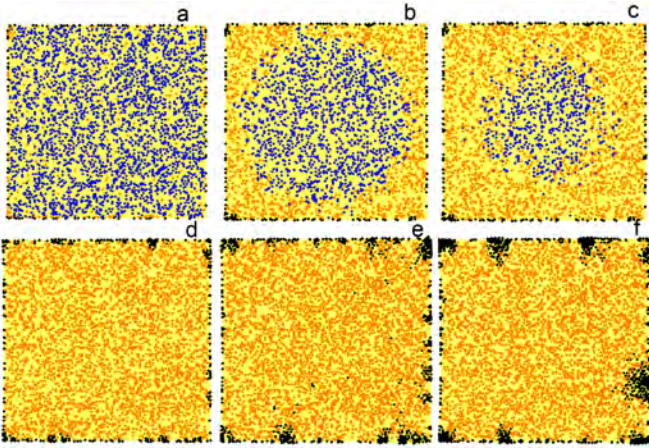


FIG. 6: Initial (upper left), intermediate and final states (lower right) after the propagation of the elastic distortion-elastic step. Yellow molecules: low spin state. Other colours: high spin molecules with a colour scale corresponding to their local pressure: black: low pressure (very stable), red: moderate pressure (stable), blue: high pressure. The snapshots correspond to situations just after photoexcitation (a), during and after the relaxation (b, c) and during fluctuations around the elastic step (d, e, f), as shown in figure 8.

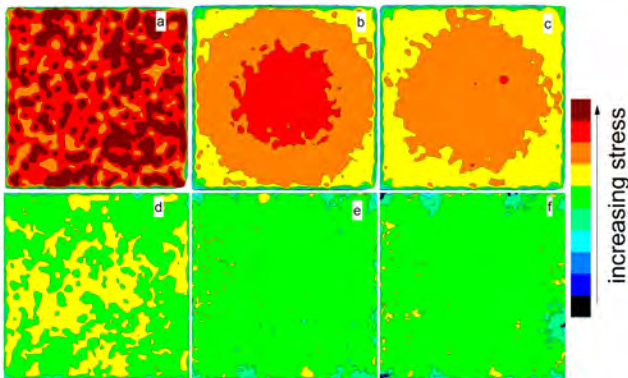


FIG. 7: Map of local pressures inside the sample during the elastic step. The snapshots correspond to those in Figure 6.

a larger elastic step. Different k entails different sound velocity, and indeed we observe that the onset of the elastic step in terms of MCES, not only its magnitude, is k dependent. The elastic step has a larger magnitude for an intermediate value of the elastic constant, as in the case of a soft lattice (low value of (k)), the local pressure is not large enough to cause the switching of many molecules, while in the case of a hard lattice (high value of (k)) the elastic distortions encounter more difficulties to propagate.³⁴

Next, we discuss the amplitude of the elastic step as a function of the ratio r between the number of steps in the differential equations solved, and the number of MCES between two successive solving of differential equation. As we have stated above, r is a measure for how fast

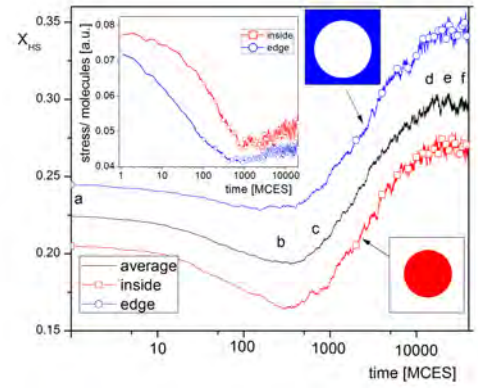


FIG. 8: Difference in the evolution of X_{HS} for central and edge regions and comparison with the average X_{HS} for the whole sample. Inset: variation of the local pressures for central and edge regions of the sample.

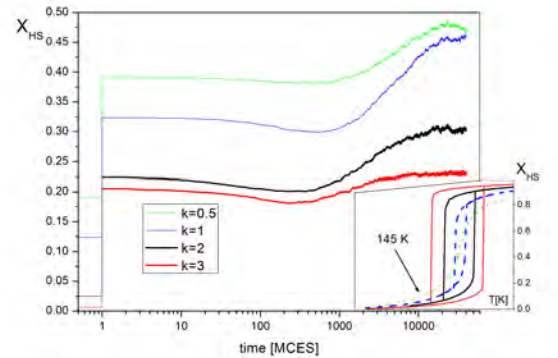


FIG. 9: The dependence of the elastic response on the elastic constant of the springs. Inset: thermal hysteresis for all elastic constants at $1000 \text{ MCsteps K}^{-1}$ — at 145 K the steady state is different for every spring constant.

is the lattice relaxation in comparison with individual molecular switching. The results for different r are presented in figure 10. If r is large then no relaxation can be observed after the photoexcitation, as the lattice relaxes (almost) completely till the next molecular switching, so the local pressure will diminish enough for all recently HS switched molecules and they will not switch back to LS . This situation corresponds to conventional LIESST experiments performed at low temperature where the photoinduced molecular HS state lives orders of magnitudes longer than the acoustic timescale. When r is somewhat smaller, the lattice does not completely relax and therefore some molecules (especially those situated in the middle of the lattice, according to figure 6) will still have a higher pressure and will switch back to LS state. This number of molecules is larger, so that is the relaxation, as r decreases more. However, in all situations, the

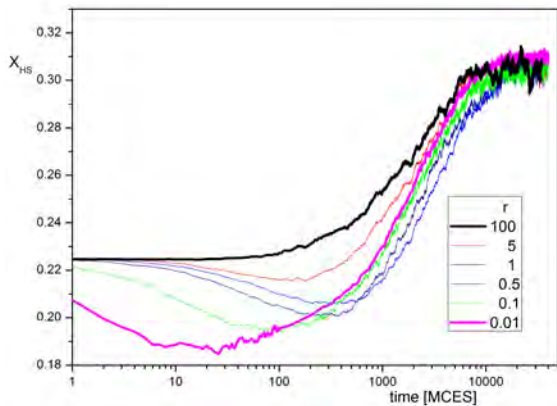


FIG. 10: The influence of the ratio probability check / steps during molecular motion on the elastic step: the temperature is considered 145 K and a 20% photoexcitation. The final state is the same irrespective to the ratio, but the initial relaxation disappears if the lattice is let to relax after every molecular change.

value of the elastic step is similar – this can be easily understood if we take into account that it is the equilibrium state for a given spin configuration. The surface shows a faster variation for larger r values, while, for smaller values, an incubation time is observed, as experimentally reported.

A final point that we would like to address is the role of the homogeneity of the photoexcitation on the value of the elastic step. It was experimentally observed that in function of various parameters, like the absorption cross section of the material, the photoexcitation wavelength or sample size, the photoexcitation can be more or less homogenous⁸. We have therefore considered different initial photoexcited state configurations, from a complete inhomogeneous one, where only the molecules near one side are photoexcited (figure 11, top) to a complete homogeneous state, where the photoexcitation is completely random, as considered in previous paragraphs. Intermediate states with the number of photoexcited molecules decreasing exponentially from one side to another have also been investigated (figure 11 bottom). The last situation would be closest to the real situation of a single crystal, of which absorption obeys Lambert-Beer law^{35,36}.

In figure 12 we show that the value of the elastic step obtained in the case of intermediate photoexcitation is three times higher than that in the case of homogeneous or inhomogeneous states, for similar global values of initial fraction of photoswitched molecules. This can be explained using the results presented in figure 10. If the photoexcitation is completely inhomogeneous and located on the surface, the photoexcited molecules will only manifest in their immediate vicinity and will not have enough force to influence distant molecules. On the other side, in the case of completely random photoexcitation, most of the photoexcited molecules will be in the bulk part of the sample, so, either they will relax

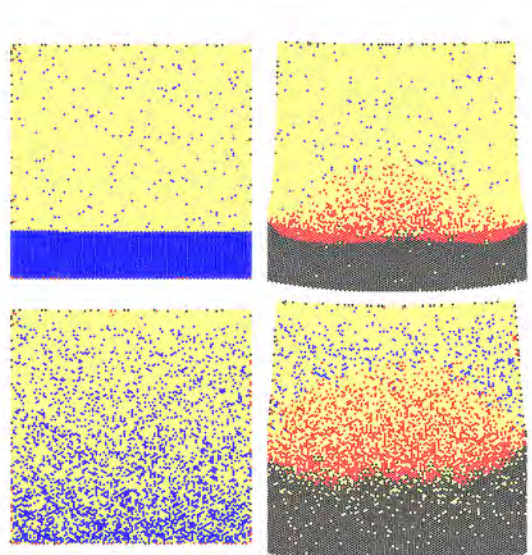


FIG. 11: Initial (left) and final state after the propagation of the elastic distortion- elastic step (right) for different initial states with 20% HS molecules. The same color scale as in figure 6 is used.

or wither they will determine the switching of a small number of LS . Therefore, the most favourable case is an intermediate one, as in figure 11 bottom. The proportion of molecules near the photoexcitation side is just high enough to determine the switching of almost all their nearby molecules, and the region till the photoexcitation population surpasses a threshold is large enough to guarantee their influence in a large part of the sample. As expected, the surface changes faster in the case of an inhomogenous state, as there are a higher number of photoexcited molecules near the edge, so the elastic distortion will need to cover a smaller distance, while for homogenous photoexcitation, the surface varies slowly.

III. CONCLUSIONS

In this paper, by using the mechanoelastic model, we have qualitatively reproduced the unusual self-amplified increase of the number of molecules in the high-spin state after femtosecond photoexcitation, recently reported in various experiments. The non-linear photo-response on acoustic timescale, for which elastic distortion propagates over the macroscopic sample, results from the competition between the local relaxation and the non-local amplification. We have explained this effect as a reorganisation of molecular states, resulting from the elastic distortion and due to the lattice deformations. Simulations points enhanced effect towards the edge and corners of the open boundary lattice. If the elastic lattice deformation origin of this self-amplification is well described by the present model, further work should consider size effects and heat

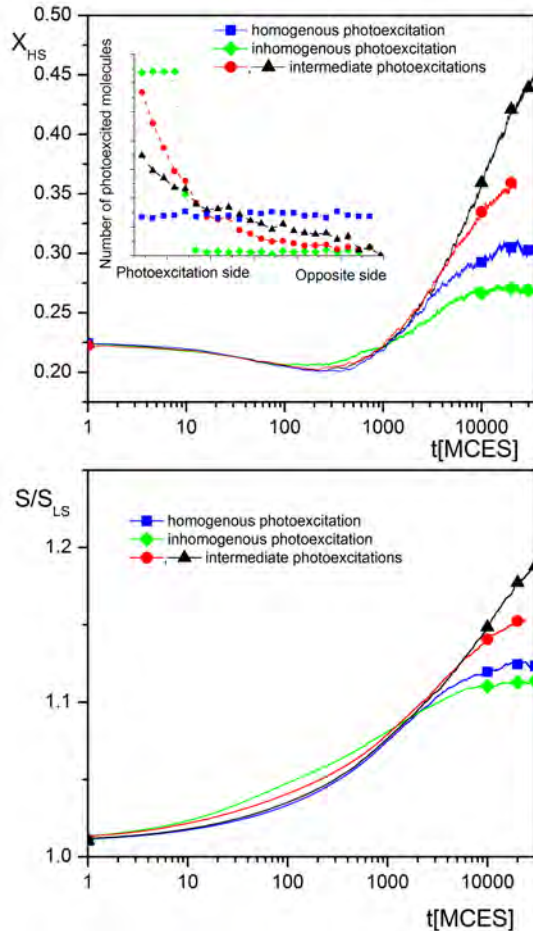


FIG. 12: The evolution of n_{HS} (up) and on the total surface (down) starting from different initial states with the same number of photoexcited molecules but with different homogeneities (see figure 11). The maximum of the elastic step is attained for an intermediate non-homogenous initial state.

propagation, which manifest at a longer timescale, of mi-

croseconds. A study of the dependence of the elastic step with the size will most likely lead to the conclusion that as the size of the crystals decreases the expansion occurs faster and elastic deformation is larger. Equally, a further study will concern the rigidity of the lattice, which may preclude amplification at low excitation density and favor it at high excitation density. Photothermal conversion is not discussed here. It depends on the proximity of the thermal phase transition, but it is limited by the thermal equilibrium timescale and energy redistribution from the photoexcited molecules to the global system should be taken into account. At least for systems homogeneously photoexcited, the description used in this paper remains valid but exponential decay of molecular temperature and exponential increase of the lattice temperature should be included. This will be a next step in our studies. Clearly one of the big hopes now is that we will be able to predict the elastic conversion time, whether it lags or not behind the volume (distortion) propagation, and that on the ultrafast time-scales for nanocrystals. We give away a taste for it in figure 11. The model can be improved by using parameters provided by ab-initio calculations such as vibration modes and frequencies or distortions during the switches between the states. We believe that the present model based on the coupling between the strain wave and the order parameter field is a new perspective extendable onto many other photoactive materials for which important molecular volume-change couple to lattice expansion^{37–42}.

Acknowledgements

This work was supported by National Research Council (CNCS-UEFISCDI), Romania, grant number PN-II-RU-TE-2014-4-0987, by the Institut Universitaire de France, Rennes Métropole, Région Bretagne (CREATE 4146), ANR (ANR-13-BS04-0002, CNRS (LIA IM-LED) and by Grants-in-Aid for Scientific Research C (No. 25400391, and No. 26400324) from MEXT of Japan.

- ¹ P. Gülich and A. Goodwin, *Spin crossover in transition metal compounds*, vol. I-III (Springer, Heidelberg, 2004).
- ² M. A. Halcrow, *Spin-crossover materials - properties and applications* (John Wiley & Sons, Chichester, UK, 2013).
- ³ E. Collet, L. Henry, L. Pineiro-Lopez, L. Toupet, and J. Real, *Current Inorg. Chem.* **6**, 61 (2016).
- ⁴ A. Marino, M. Buron-Le Cointe, M. Lorenc, L. Toupet, R. Henning, A. D. DiChiara, K. Moffat, N. Brefueld, and E. Collet, *Faraday Discuss.* **177**, 363 (2015).
- ⁵ R. Bertoni, M. Lorenc, H. Cailleau, A. Tissot, J. Laisney, M. Boillot, L. Stoleriu, A. Stancu, C. Enachescu, and E. Collet, *Nat. Mater.* **15**, 606 (2016).
- ⁶ R. Bertoni, M. Lorenc, T. Graber, R. Henning, K. Moffat, J. Letard, and E. Collet, *Cryst. Eng. Comm.* (2016).

- ⁷ R. Bertoni, M. Lorenc, A. Tissot, M. L. Boillot, and E. Collet, *Coord. Chem. Rev.* **282**, 66 (2015).
- ⁸ E. Collet, N. Moisan, C. Balde, R. Bertoni, E. Trzop, C. Laulhe, M. Lorenc, M. Servol, H. Cailleau, A. Tissot, et al., *Phys. Chem. Chem. Phys.* **14**, 6192 (2012).
- ⁹ E. König, *Struct. Bonding* **76**, 51 (1991).
- ¹⁰ A. Hauser, *Top. Curr. Chem.* **234**, 155 (2004).
- ¹¹ S. Decurtins, P. Gülich, C. P. Kohler, H. Spiering, and A. Hauser, *Chem. Phys. Lett.* **10**, 1 (1984).
- ¹² A. Hauser, *Chem. Phys. Lett.* **192**, 65 (1992).
- ¹³ R. Bertoni, M. Lorenc, A. Tissot, M. Servol, M. Boillot, and E. Collet, *Angew. Chem. Int. Ed.* **51**, 7485 (2012).
- ¹⁴ M. Lorenc, J. Hebert, N. Moisan, E. Trzop, M. Servol, M. Buron-Le Cointe, H. Cailleau, M. L. Boillot, E. Pon-

- tecorvo, M. Wulff, et al., *Phys. Rev. Lett.* **103**, 028301 (2009).
- ¹⁵ A. Marino, M. Cammarata, S. F. Matar, J. F. Letard, G. Chastanet, M. Chollet, J. M. Glowina, H. T. Lemke, and E. Collet, *Struct. Dynam. US* **3**, 028301 (2016).
- ¹⁶ R. Bertoni, M. Cammarata, M. Lorenc, S. F. Matar, J. F. Letard, H. T. Lemke, and E. Collet, *Accounts Chem. Res.* **48**, 774 (2015).
- ¹⁷ M. Cammarata, R. Bertoni, M. Lorenc, H. Cailleau, S. Di Matteo, C. Mauriac, S. F. Matar, H. Lemke, M. Chollet, S. Ravy, et al., *Phys. Rev. Lett.* **113**, 227402 (2014).
- ¹⁸ E. Collet, M. Lorenc, M. Cammarata, L. Guerin, M. Servol, A. Tissot, M. L. Boillot, H. Cailleau, and B.-L. C. M., *Chem.-Eur. J.* **18**, 2051 (2012).
- ¹⁹ Y. Konishi, H. Tokoro, M. Nishino, and S. Miyashita, *Phys. Rev. Lett.* **100**, 067206 (2008).
- ²⁰ M. Nishino, K. Boukheddaden, Y. Konishi, and S. Miyashita, *Phys. Rev. Lett.* **98**, 247203 (2007).
- ²¹ M. Nishino, C. Enachescu, S. Miyashita, P. A. Rikvold, K. Boukheddaden, and F. Varret, *Sci. Rep.* **1**, 162 (2011).
- ²² W. Nicolazzi, S. Pillet, and C. Lecomte, *Phys. Rev. B* **78**, 174401 (2008).
- ²³ C. Enachescu, L. Stoleriu, A. Stancu, and A. Hauser, *Phys. Rev. Lett.* **102**, 257204 (2009).
- ²⁴ C. Enachescu, M. Nishino, S. Miyashita, K. Boukheddaden, F. Varret, and P. A. Rikvold, *Phys. Rev. B* **91**, 104102 (2015).
- ²⁵ C. Enachescu, L. Stoleriu, A. Stancu, and A. Hauser, *Phys. Rev. B* **82**, 104114 (2010).
- ²⁶ E. Holmstrom and L. Stixrude, *Phys. Rev. Lett.* **114**, 117202 (2015).
- ²⁷ K. Bairagi, O. Iasco, A. Bellec, A. Kartsev, D. Li, J. Lagoute, C. Chacon, Y. Girard, S. Rousset, F. Miserque, et al., *Nature Comm.* **7**, 12212 (2016).
- ²⁸ P. Chakraborty, C. Enachescu, and A. Hauser, *Eur. J. Inorg. Chem.* **5-6**, 770 (2013).
- ²⁹ M. Nishino, T. Nakada, C. Enachescu, K. Boukheddaden, and S. Miyashita, *Phys. Rev. B* **88**, 094303 (2013).
- ³⁰ C. Enachescu and A. Hauser, *Phys. Chem. Chem. Phys.* **18**, 20591 (2016).
- ³¹ M. Lorenc, C. Balde, W. Kaszub, A. Tissot, N. Moisan, M. Servol, M. Buron-Le Cointe, H. Cailleau, P. Chasle, P. Czarnecki, et al., *Phys. Rev. B* **85**, 054302 (2012).
- ³² H. Cailleau, M. Lorenc, L. Guerin, M. Servol, E. Collet, and M. Buron-Le Cointe, *Acta Cryst.* **A66**, 189–197 (2010).
- ³³ See Supplemental Material at [URL will be inserted by publisher] for a movie presenting the evolution of a system during the elastic step. Color scale in the movie: blue: LS molecules, yellow: HS molecules with high pressure, red: HS molecules with low pressure).
- ³⁴ A. Slimani, K. Boukheddaden, and K. Yamashita, *Phys. Rev. B* **92**, 014111 (2015).
- ³⁵ D. B. Judd and G. Wyszecski, *Color in Business, Science and Industry* (Wiley, New York, 1975).
- ³⁶ C. Enachescu, F. Varret, E. Codjovi, J. Linares, S. Floquet, P. Manikandan, and P. T. Manoharan, *J. Phys. Chem. B* **110**, 5883 (2006).
- ³⁷ S. Kobatake, S. Takami, H. Muto, T. Ishikawa, and M. Irie, *Nat.* **446**, 778 (2007).
- ³⁸ S. Ohkoshi, Y. Tsunobuchi, T. Matsuda, K. Hashimoto, A. Namai, F. Hakoe, and H. Tokoro, *Nat. Chem.* **2**, 539 (2010).
- ³⁹ A. Camjayi, C. Acha, R. Weht, M. G. Rodriguez, B. Corraze, E. Janod, L. Cario, and M. J. Rozenberg, *Phys. Rev. Lett.* **113**, 086404 (2014).
- ⁴⁰ H. Okamoto, Y. Ishige, S. Tanaka, H. Kishida, S. Iwai, and Y. Tokura, *Phys. Rev. B* **70**, 165202 (2004).
- ⁴¹ Y. Okimoto, X. Peng, M. Tamura, T. Morita, K. Onda, T. Ishikawa, S. Koshihara, N. Todoroki, T. Kyomen, and M. Itoh, *Phys. Rev. Lett.* **103**, 027402 (2009).
- ⁴² S. Cobo, D. Ostrovskii, S. Bonhommeau, L. Vendier, G. Molnar, L. Salmon, K. Tanaka, and A. Bousseksou, *J. Am. Chem. Soc.* **130**, 9019 (2008).